Extended Abstracts of the 2006 International Conference on Solid State Devices and Materials, Yokohama, 2006, pp. 1062-1063

H-9-4

# Analytical Model for Phonon-Limited Mobility in n-MOS Inversion Layers on Arbitrarily Oriented and Strained Si Surfaces

Mélanie Szczap[1,2], Nicolas Cavassilas[1], Frédéric Boeuf[2], Fabrice Payet[2] and Thomas Skotnicki[2]
[1]L2MP, CNRS, UMR 6137, Bât. IRPHE, Technopôle de Château-Gombert, 13384 Marseille Cedex 13
Phone: +33(0)4 96 13 97 26 E-mail: nicolas.cavassilas@l2mp.fr
[2]STMicroelectronics, 850 rue Jean Monnet, 38920 Crolles Cedex, France

## 1. Introduction

The electron mobility enhancement with strain can be explained by the subband structure in inversion layer and by modification of phonon scattering. Models proposed in previous works use Boltzmann transport equation and/or Schrödinger-Poisson solver [1], that are not compatible with compact models.

In this paper, we present a completely analytical model for electron mobility ($\mu_e$) in strained Si inversion layers. The electronic states in the inversion layer are calculated in the Airy approximation of the triangular quantum well, and the relaxation times are evaluated with a novel analytical model depending on only one parameter. As a result, this model enables the calculation of $\mu_e$ in arbitrarily oriented and strained Si surfaces, with any channel direction. Results of $\mu_e$ in strained and unstrained Si are in good agreement with experimental and theoretical [2, 3] data.

## 2. Modeling the Electron Mobility

As an input of our model, we calculate the complete band structure of the strained semiconductor (Fig. 1) to obtain the conduction band splitting $\Delta E_{strain}$ and the electron effective masses. In this aim, we use a 30 band **k.p** Hamiltonian taking into account spin-orbit coupling [4]. Note that the mobility model we propose is completely independent of the way conduction masses are calculated, so that any other method for calculating the band structure could be used. The masses in the direction of confinement $m_{conf}$ and the density-of-states masses $m_{DOS}$ are calculated with the method of the reciprocal effective-mass tensor [5]. Fig. 2 shows a schematic representation of the constant-energy ellipses for the (001), (110) and (111) surfaces of Si, and their associated effective masses $m_{conf}$ and $m_{DOS}$. The conductivity mass $m_c^*$ along the transport direction $\theta$ (see Fig. 2) is defined as the curvature of the conduction band in this direction.

In a second step, the two-dimensional nature of electron gas in the inversion layer is considered. The subband energies, the envelope function of the eigenstates, and the surface carrier proportion $n_{ij}$ in the i^th^ subband of the valley j are calculated in the Airy approximation of the triangular quantum well. Although it is not applicable at high effective fields and doping levels, this approach is completely analytical. Moreover, improvement can be obtained using the analytical model described in [6].

The last step for the evaluation of electron mobility is to calculate the relaxation times. Only phonon scattering is taken into account in our calculation of mobility since it is the dominant mechanism for inversion mobility near room temperature. Then, with physical considerations about transport mechanisms in an inversion layer at low field, we could derive analytical expressions of the relaxation times. The total relaxation time $\tau_{ij}^{eff}$ for the ith subband of the valley j is expressed as:

$$\frac{1}{\tau_{ij}^{eff}} = \frac{1}{\tau_j}\frac{W_{ij}}{L_j} \qquad (1)$$

where $W_{ij}$ is the effective width of the inversion layer for the ith subband of the valley j, and depends on the form of the envelope function, and $L_j$ is de Broglie wavelength of the valley j, and depends on the mass $m_{conf,j}$. The relaxation time $\tau_j$ is given by:

$$\tau_j = \tau_{ref}\frac{m_{DOS,ref}}{\sqrt{m^*_{c,ref}(\theta=0)}}\frac{\sqrt{m^*_{c,j}(\theta=0)}}{m_{DOS,j}}\sqrt{\frac{m^*_{c,j}(\theta)}{m^*_{c,j}(\theta=0)}} \qquad (2)$$

where the index *ref* refers to a reference valley. The two first ratios in (2) make $\tau_j$ depend on the surface orientation, while the last ratio makes $\tau_j$ depend on the in-plane channel direction $\theta$. Thus, with only one fitting parameter $\tau_{ref}$, we can calculate $\tau_{ij}^{eff}$ for different surface orientations, in-plane channel directions and types of strain. Finally, according to carrier proportions in each subband of each valley calculated in the Airy approximation, the effective mobility is given by:

$$\mu_{eff} = \sum_i\sum_j n_{ij}.\mu_{ij}^{eff} \quad \text{with} \quad \mu_{ij}^{eff} = \frac{q\,\tau_{ij}^{eff}}{m^*_{c,j}} \qquad (3)$$

## 3. Results and Discussion

First, the effect of surface orientation on phonon-limited electron mobility in unstrained-Si, is investigated. We obtain a mobility in good agreement with universal mobility for effective fields ranging from 0.1 MV/cm up to 2 MV/cm. Results in Fig. 3 show that mobility on a (110) surface is greater than mobility on (001) and (111) surfaces. This can be explained by the fact that the masses responsible for the transport in the confined valleys of (110)-Si are the smallest – in comparison with the other surface orientations - while the carrier proportions in these valleys are the highest. These results do not explain experimental data obtained by [7] and [8] since we do not include surface roughness effects, but they are of the same magnitude order. Then, we study the effect of channel orientation, and Fig. 4 shows the anisotropy of mobility on (110), whereas mobility on (001) and (111) surfaces is isotropic. In this configuration, the best phonon-limited mobility on Si(110) is obtained for <001> channels.

In order to quantitatively examine the influence of strain on the electron mobility, we study two types of strain: bi-axial strain and uni-axial strain parallel to <100> on (001)-Si. In Fig. 5 it is observed that mobility enhancement is greater with a bi-axial tensile strain than with a uni-axial tensile strain, as showed in [9]. Moreover, mobility enhancement decreases as the effective field, thus confinement increases (cf. Fig. 6 and 7), showing that measured gains in small devices cannot be explained by considering only phonon scattering. The impact of channel orientation under a <100> uni-axial tensile strain on mobility is illustrated in Fig. 8 showing that mobility enhancement with a <100> channel is higher than with a <110> channel. Finally, the impact of CESL layer on mobility is assessed, using a layout-dependant deformation tensor calculated from TCAD simulations. Results (Fig. 9) are also found to be in good agreement with [10].

An application of our model to device performance calculation can be performed using the MASTAR model [11]. Example of the impact CESL impact on nMOS Idsat using mobility calculated in Fig.9 is shown in Fig. 10.

## 4. Conclusions

A novel analytical model for phonon-limited electron mobility in inversion layers is proposed. Electron mobility is evaluated fully analytically with only one fitting parameter, and results are in good agreement with experimental and theoretical data for different device configurations. This model enables device engineers to perform quick predictions for various key technologies. Performances obtained with other materials such as Ge and device architectures should also be investigated with this model.

## Acknowledgements

This work was partially supported by E.U. Project SiNANO and NanoCMOS.

## References

[1] S.-i. Takagi, *et al.*, J. Appl. Phys., **80**(1996)1567.
[2] K. Uchida, *et al.*, IEDM Tech. Digest. (2004)229.
[3] J. J. Welser, *et al.*, IEDM Tech. Digest. (1994)373.
[4] S. Richard, *et al.*, Phys. Rev. B, **70**(2004)235204.
[5] F. Stern and W. E. Howard, Phys. Rev., **163**(1967)816.
[6] M. Ferrier, *et al.*, Solid-State Electron., **50**(2006)69-77.
[7] M. Yang, *et al.*, IEDM Tech. Digest. (2003)453.
[8] H. Irie, *et al.*, IEDM Tech. Digest. (2004)225.
[9] K. Uchida, *et al.*, IEDM Tech. Digest. (2005).
[10] F. Lime, *et al.*, ESSDERC Tech. Digest. (2005).
[11] T. Skotnicki and F. Boeuf, ECS conference Tech. Digest. (2002)720.

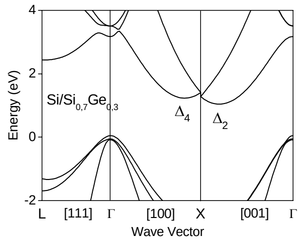

Figure 1: Band structure of strained Si on $Si_{0.7}Ge_{0.3}$ calculated with a 30 band k.p Hamiltonian.

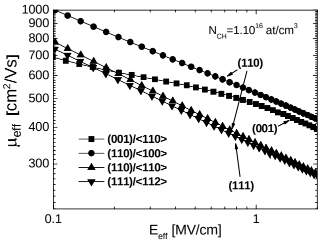

Figure 3: Electron mobility as a function of effective field at $N_{ch} = 1{\times}10^{16}$cm$^{-3}$, for Si (001), (110) and (111).

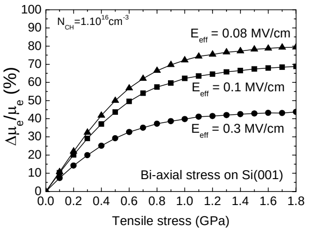

Figure 7: Mobility enhancement as a function of strain at $N_{ch} = 1{\times}10^{16}$cm$^{-3}$, for various effective fields. The gain decreases faster as $E_{eff}$ increases.

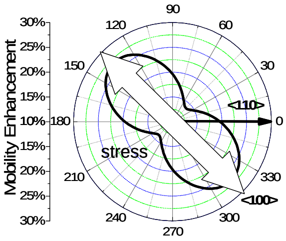

Figure 8: Mobility enhancement under a <100> uni-axial tensile stress of 1GPa, as a function of channel orientation, for a (001) surface ($N_{ch}$=1×10$^{16}$cm$^{-3}$).

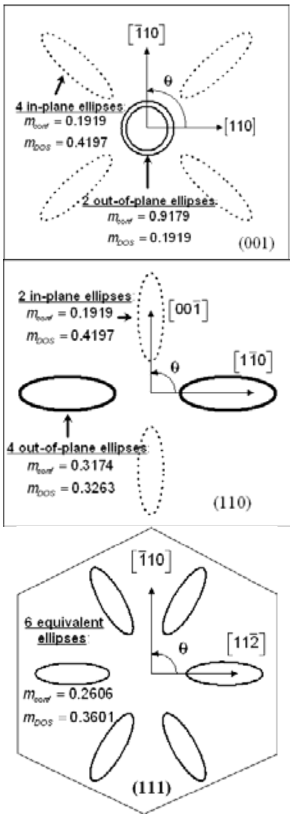

Figure 2: Schematic representation of the constant-energy ellipses for the (001), (110) and (111) surfaces of Si, and their associated effective masses $m_{conf}$ and $m_{DOS}$. $\theta$ is the in-plane off angle determining the transport direction.

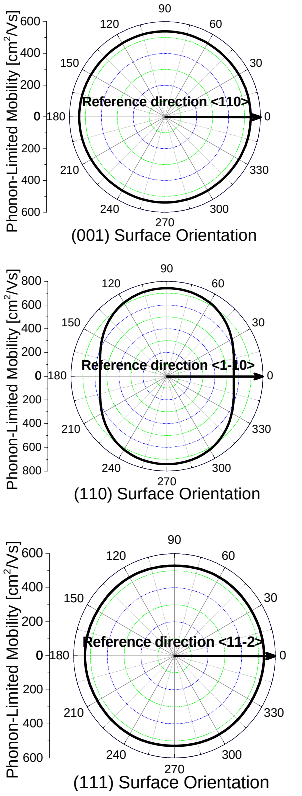

Figure 4: Channel direction dependence of mobility for electrons on unstrained Si(001), (110) and (111) doped with $N_{ch}$=1×10$^{16}$cm$^{-3}$. $N_{inv}$=3×10$^{12}$cm$^{-2}$. Mobilities on Si(001) and (111) are isotropic, whereas mobility on Si(110) is anisotropic.

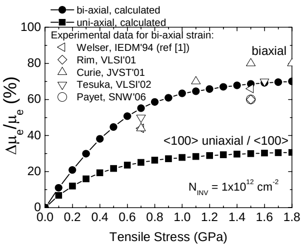

Figure 5: $\mu_e$ enhancement on Si(001) as a function of strain at $N_{ch} = 1{\times}10^{16}$cm$^{-3}$. Bi-axial stress is better than uni-axial stress.

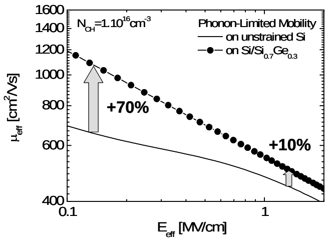

Figure 6: Mobility enhancement decreases as effective field increases (e.g. with Si on $Si_{0.7}Ge_{0.3}$).

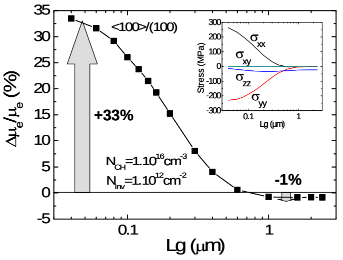

Figure 9: $\mu_e$ enhancement under a tensile CESL layer. For short Lg, maximum stress components are $\sigma_{xx}$=260MPa and $\sigma_{yy}$=-230MPa (see inset figure).

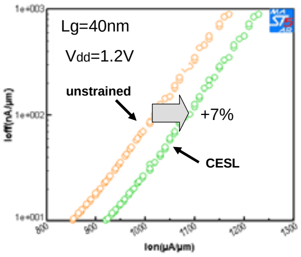

Figure 10: impact of $\mu_e$ enhancement by CESL on device performance evaluated through MASTAR model.